Chalcogenide Letters Vol. 11, No. 9, September 2014, p. 425- 431

# ELECTRODEPOSITION OF CdSe LAYERS OF VARIOUS THICKNESS TO IMPROVE THE PHOTOCATALYTIC PERFORMANCE OF THE CdS/CdSe BILAYER STRUCTURE

C. LU[a], L. ZHANG[a,b,*], Y. ZHANG[a], S. LIU[a], G. LIU[a,c]
[a]*Science and Technology on Plasma Physics Laboratory, Research Center of Laser Fusion, China Academy of Engineering Physics, Mianyang, China*
[b]*Jointment Laboratory for Extreme Conditions Matter Properties, Southwest University of Science and Technology Research Center of Laser Fusion, China Academy of Engineering Physics, Mianyang, China*
[c]*School of Chemical Engineering and Technology, Harbin Institute of Technology, Harbin 150001, China*

CdS thin films were prepared using the chemical bath deposition (CBD) process and annealed in argon atmosphere. The grain size and light absorbance increased after annealing. The CdSe layer was electrodeposited on a CdS film galvanostatically employing various for deposition times. The resulting films were studied using XRD, FESEM, UV-Vis spectroscopy and electrochemical impedance spectroscopy to characterize their structural, morphological, and photoelectrochemical characteristics. The resulting CdS/CdSe bilayer structure exhibits significant enhancements in optical absorption, photocurrent density, and photoconversion efficiency. In particular, the CdS/CdSe (6 min) sample exhibited a maximum photocurrent density of 8 mA/cm$^2$ and maximum photoconversion efficiency of 4.90%.

(Received August 13, 2014; Accepted September 18, 2014)

*Keywords:* CdS/CdSe; Photocatalysis; CBD; Electrodeposition; Multilayer structure

## 1. Introduction

Cadmium sulfide (CdS) and cadmium selenide (CdSe) are typical II-IV group semiconductors. Because they have a direct energy band gap (2.42 eV of CdS, 1.70 eV of CdSe) and high electron mobility (200 cm$^{-2}$/V·s and 800 cm$^{-2}$/V·s) [1, 2], these materials are used widely in many applications, such as luminescence, biosensor, solar cells and as photocatalysts [3]. Due to their narrow band gaps and relatively negative potentials valence band, they exhibit excellent absorption properties in the visible light region, which affords them good photocatalytic activity under visible light radiation [4-5]. According to the literature, CdS and CdSe are used as sensitizers when combined with other semiconductors in photocatalytic and solar cell applications. For example, when CdS or CdSe is combined with $TiO_2$, ZnS, ZnO, CdO, and these cascade structures exhibit enhancement in their optical absorption property and photocatalytic performance [6-9].

In this study, in order to determine the effect of CdSe layer thickness on the photocatalytic performance of CdS/CdSe bilayer structure, CdS films were prepared using CBD and a CdSe layer was overlain on the CdS films using galvanostatically with different deposition times, resulting in CdS/CdSe bilayer structures. The crystal structure of the films was examined using XRD. The morphology and thickness of films was characterized by FESEM, while the absorption spectra

* Corresponding author: roger0314@163.com

were measured using a UV-Vis spectroscopy. The photocatalytic performances and electrochemical impedance spectroscopy (EIS) were tested under light illumination of one sun.

## 2. Experimental Details

The initial CdS film layer were deposited on ITO coated glass using chemical bath deposition (CBD). The chemical bath contained 0.005 M $CdCl_2$, 0.01 M $(NH_2)_2SC$ and 0.05 M $NH_4Cl$ and the pH value was adjusted to 10.5 with $NH_3 \cdot H_2O$. The solution was heated to 80 °C which resulted in CdS films on the substrate after for 2 hours of immersion in the solution. The resulting films were annealed in argon at 250 °C for 2 hours. In the next step the CdS/CdSe bilayer structure was formed by galvanostatically electrodepositing a CdSe layer over the on CdS substrate using a Reference 600 electrochemical workstation (GAMRY Instruments). For this work, the electrolyte contained 0.1 M $CdCl_2$ and 0.01 M $SeO_2$ with a pH of 2, adjusted with hydrochloric acid. Electrodeposition was employed in a three-electrode setup consisting of an Ag/AgCl (saturated KCl) reference electrode, a Pt-sheet counter electrode (2 cm × 2 cm), and an ITO coated glass substrate as a working electrode (1 cm × 2 cm). The deposition current density was set as -4 $mA/cm^2$. The different thicknesses of the CdSe layers were obtained by varying the deposition time. The crystal forms of the product films were determined by XRD (Rigaku Ultima IV diffractometer) with Cu Kα radiation (λ= 1.5406Å). The morphology and thickness of films were characterized by FESEM (FEI Inspect F50). An UV-Vis spectrophotometer (PerkinElmer Lambda 950) was used to analyze the light absorption properties of films. The photocatalytic performance of the films was characterized using a photoelectrochemical cell with Pt-sheet counter electrode and saturated calomel electrode (SCE) reference electrode. The measurements were tested under illumination (AM1.5 100 $mW/cm^2$) in an electrolyte composed of 0.35 M $Na_2S_2O_3$ and 0.25 M $Na_2S$. EIS was performed from an initial frequency of 100 kHz to a final frequency of 1 Hz under illumination employing the same electrochemical cell and electrolyte.

## 3. Results and Discussion

### 3.1 Characterization of CdS and CdS/CdSe thin films

The X-ray diffraction patterns of these films are displayed in Fig. 1. The patterns confirmed that both CdS and CdSe films had a cubic zinc blende phase. This was verified by matching the CdS and CdSe patterns with JCPDS card 80-0019 and 88-2346. As seen in Fig. 1, an intense peak at $2\theta = 26.75°$ in the CdS pattern is associated with the plane (1 1 1), while the peak, located at $2\theta = 25.47°$ in the CdSe pattern is the characteristic peak of CdSe plane (1 1 1). The red plot is of the annealed CdS film's XRD pattern. Compared with the unannealed CdS film, the orientation of the (1 1 1) plane of the annealed CdS haa intensified. This indicates that the grain size of CdS increased following annealing. The crystallite size can be calculated from the XRD pattern using Scherer formula: $D = 0.9\lambda/\beta\cos\theta$ [10], where D is the crystalline diameter, λ is the wavelength of the incident radiation, β is the full width at half maximum and θ is the Bragg angle. The calculated average grain sizes of the CdS film before and after annealing are 29 nm and 42 nm, respectively.

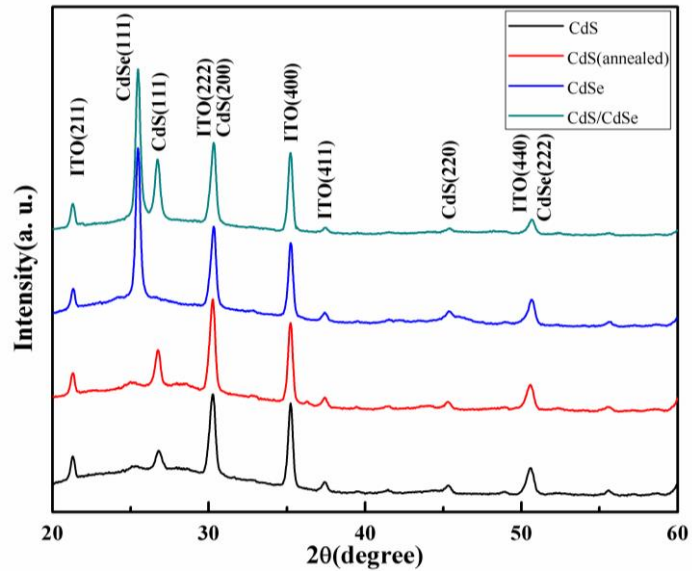


*Fig. 1 The XRD patterns of samples.*

The surface morphology and cross section of CdS and CdS/CdSe bilayer structure was examined using SEM (Fig. 2). Compared with unannealed CdS, the annealed CdS surfaces are smoother and the boundaries between grains are more blurred. The SEM image confirmed that the grain size increased after annealing. The electrodeposited CdSe is shown in Fig. 2(c), the surface topography of CdSe is smoother than that of the CdS thin film and the crystal grains are smaller. The cross section of CdS/CdSe (3 min) bilayer structure is displayed in Fig. 2(d), this sample clearly exhibits the ITO/CdS/CdSe three-layered structure. The thickness of each layer can be measured from the SEM image, which revealed that the CdS and CdSe layers thickness were 220 nm and 330 nm, respectively. This indicated that the electrodeposition method was more conducive to the growth of thin films. The relationship between the deposition time and thickness of CdSe layer are presented in Table 1.

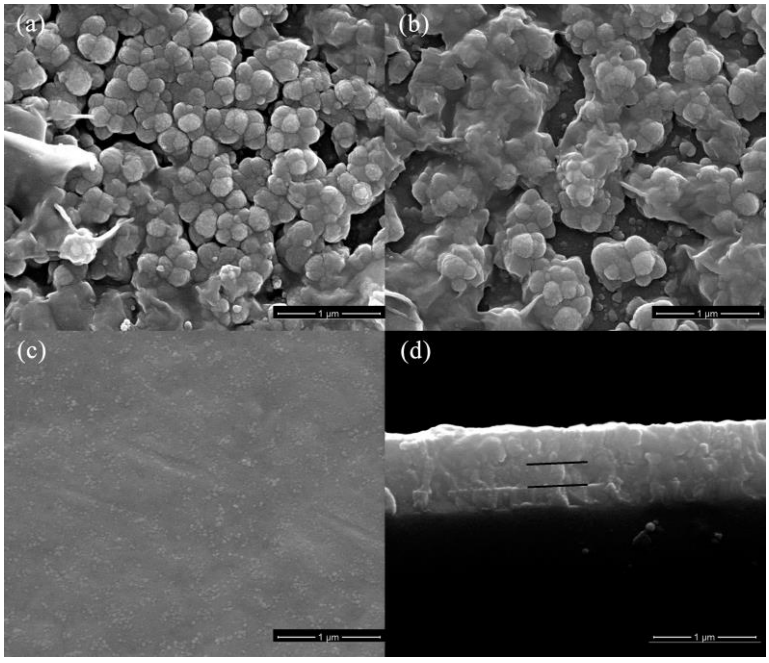


*Fig. 2 SEM images of samples. (a) CdS; (b) CdS(annealed); (c) CdSe; (d) cross section of ITO/CdS/CdSe.*

*Table 1 The relationship between the deposition time and the thickness of CdSe layer.*

| Deposition time (min) | Thickness (nm) |
|---|---|
| 2 | 260 |
| 3 | 330 |
| 4 | 385 |
| 5 | 445 |
| 6 | 490 |

The optical absorption property of films was investigated using UV-Vis spectroscopy and the spectra are displayed in Fig. 3. The CdS thin film, which was annealed in argon, exhibited better absorbance than unannealed CdS film in the visible light area. This result seems to explain why the annealed CdS film had a larger photocurrent density than unannealed film. The absorption spectra of the CdS/CdSe films with various thickness of CdSe were also determined. The film's absorption coefficient increased with the increase of film thickness in the wavelength region of 300 nm to 600 nm. When the CdSe layer was electrodeposited on CdS substrate, the maximum absorption coefficient of the two layered film increased from 2 to 2.7. When the deposition time was 6 min, the CdSe layer thickness is 495 nm (Table 1) and the CdS/CdSe film had the maximum absorbance of 4.3.

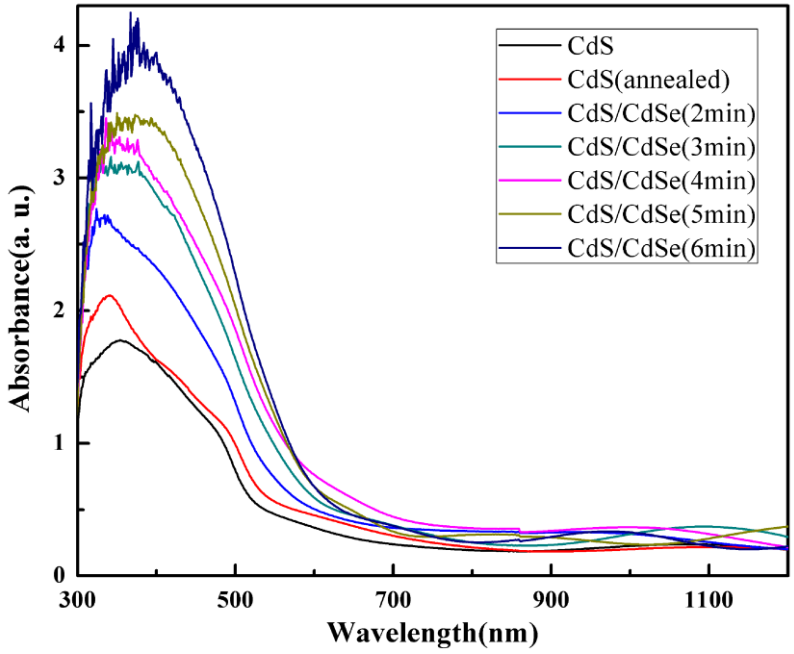


*Fig. 3 The UV-vis absorption spectrums of samples.*

### 3.2 Photocatalytic activity of CdS and CdS/CdSe thin films

The photocurrent density of the CdS and CdS/CdSe bilayer were determined, the test results are shown in Fig. 4. As the same with absorption spectrums results, the photocurrent density was enhanced by an increase in the CdSe layer thickness. Compared with unannealed CdS film, the photocurrent density of annealed CdS film increased from 1 to 1.5 mA/cm$^2$, indicating that the thermal annealing improved the film morphology. As seen in Fig. 4(a), when the 2 min

deposition time for the CdSe layer on the annealed CdS film dramatically increased the photocurrent density which reached 4 mA/cm$^2$. The CdS/CdSe(6 min) film attained a maximum photocurrent of about 8 mA/cm$^2$. The photoresponse behavior of these films is displayed in Fig. 4(b). The film was very photosensitive and responded quickly to the presence of absence (witching on and off) of light. The photocurrent density exhibited less attenuation as time increased, which might be related to the film's photocorrosion in the test solution. The photoresponse results indicated that the photo-generated current and charge transport of these films was rapidly reproduced.

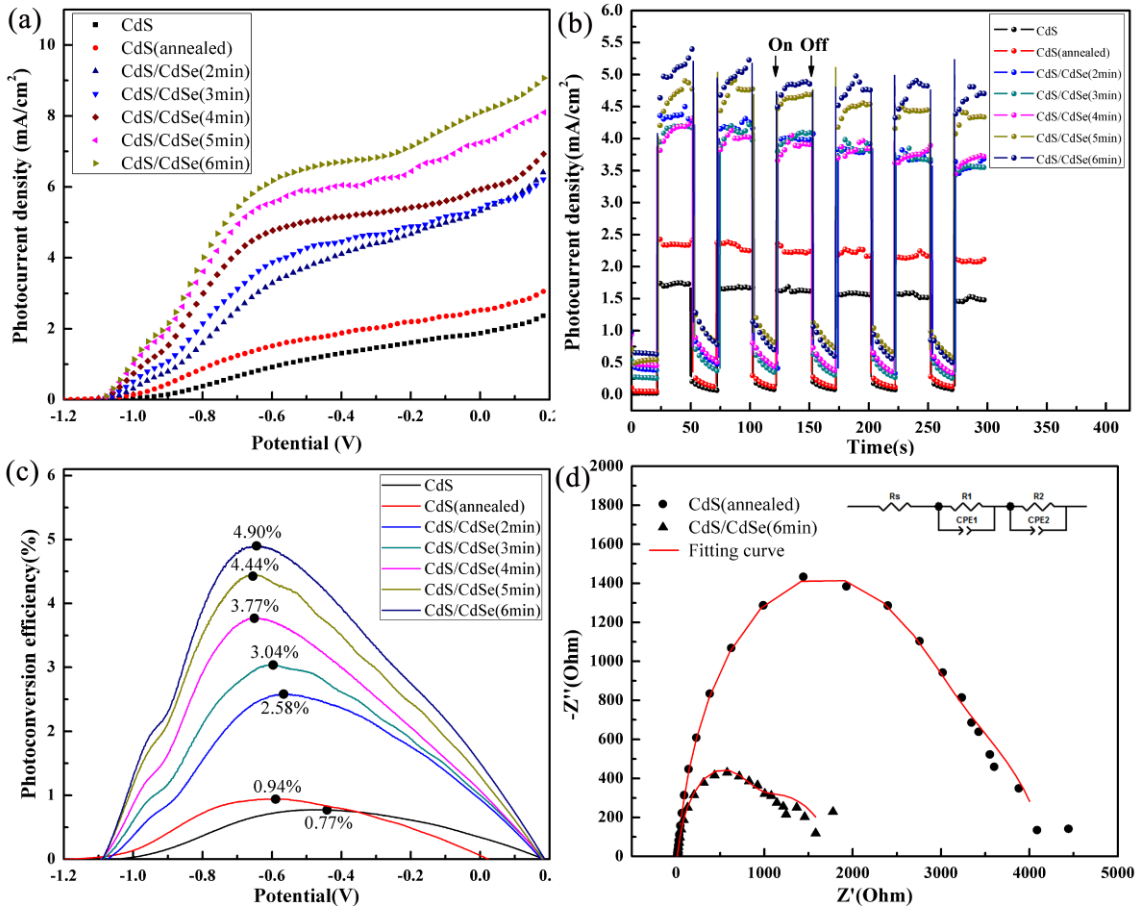


*Fig. 4 The photoelectrochemical properties of samples under illumination. (a) photocurrent density; (b) photoresponse under pulse illumination; (c) photoconversion efficiency; (d) EIS spectra.*

The photoconversion efficiency of light energy to chemical energy was calculated and is presented in Fig. 4(c). This was obtained using the following expression [8, 11-13]:

$$\eta(\%) = \frac{j_p[(E^0_{rev} - |E_{app}|)]}{I_0} \times 100$$

where $j_p$ is the photocurrent density in mA/cm$^2$, and $I_0$ is intensity of incident light in mW/cm$^2$. $E^0_{rev}$ is the standard reversible potential which is 1.23 V (vs. SCE). $E_{app} = E_{meas} - E_{aoc}$, where the $E_{meas}$ is the electrode potential (vs. SCE) of the working electrode, which is measured under

illumination of light at different photocurrent. And the $E_{aoc}$ is the electrode potential (vs. SCE) of the same working electrode at open-circuit condition under same illumination and in the same electrolyte solution. The annealed CdS sample achieved a photoconversion efficiency of 0.94%. The photoconversion efficiency was enhanced to 2.58% when a 2 min CdSe layer was deposited on CdS substrate. As deposition time increased, the photoconversion efficiency also increased and CdS/CdSe (6 min) sample obtained a maximum efficiency of 4.90% of the samples investigated. This photoconversion efficiency value of 4.90 % is a 5 times enhancement over that of the annealed CdS film.

Electrochemical impedance spectroscopy (EIS) analysis of the experimental films was measured under the illumination. The Nyquist plots for the annealed CdS and CdS/CdSe(6 min) samples are shown in Fig. 4(d). Because the first semicircle in these two electrodes merged with the second semicircle, it hardly appeared in the spectrum. A simplified equivalent circuit was used to fit impedance spectroscopy measurements of two samples and it is displayed as an inset in Fig. 4(d). It consists of $R_s$, $R_1$, $R_2$ and $CPE_1$ and $CPE_2$ elements. Where $R_s$ is the series resistance, $R_1$ is the recombination resistance, $CPE_1$ is a constant phase element representing the chemical capacitance, $R_2$ represents the charge transfer resistance between the counter electrode and the redox couple. The $CPE_2$ element takes into account the capacitance of the electrolyte-counter electrode interface [14-17]. The low frequency semicircle contained the chemical capacitance of CdS or CdS/CdSe bilayer structure and charge transfer resistance between CdS or CdS/CdSe bilayer and the electrolyte. In contrast to the CdS monolayer electrode, the CdS/CdSe structure had lower charge transfer resistance which might be related to the higher photocurrent density of the CdS/CdSe sample.

## 4. Conclusion

The objective of this research was to fabricate bilayers of CdS and CdSe to improve the photovoltaic properties of CdS. To accomplish this, CdS films first deposited onto ITO substrates using a chemical bath deposition method and the product was thermally annealing in Ar to remove internal stress. Following annealing, both the grain size and light absorption coefficient of CdS films increased. CdSe layers were then deposited on the CdS films using an electrodeposition method employing various deposition times. These CdS/CdSe bilayer films were characterized by UV-Vis spectroscopy and SEM, which revealed a three-layer ITO/CdS/CdSe structure. Finally, the photoelectrochemical properties of the subject films were evaluated under illumination. These results revealed that as the CdSe layer thickness increased, the photocurrent density and photoconversion efficiency of the film also increased. The 6 minutes deposition CdS/CdSe sample exhibited the maximum photocurrent density and photoconversion efficiency of 8 $mA/cm^2$ and 4.90%, respectively. Electrochemical impedance spectroscopy of the films revealed that the bilayer films exhibited lower charge transfer resistance which might be the reason for the higher photocurrent density of the CdS/CdSe samples.

**Acknowledgment**

The authors acknowledge the supports by Science and Technology Development Foundation of China Academy of Engineering Physics (No. 2012A0302015 and No. 2012B0302050), and Key Laboratory of Ultra Precision Machining Technology of China Academy of Engineering Physics (No. ZZ13019).

## References

[1] K. Zarębska, M. Skompska. Electrochim. Acta, **56**, 5731 (2011).
[2] F. F. Andrew, E. C. Carroll, D. S. Larsen, et al. Chem. Commun., **44**, 2206 (2008).
[3] S. M. Pawar, A.V. Moholkar, C. H. Bhosale. Mater. Lett., **61**, 1034 (2007).
[4] M. R. Gao, Y. F. Xu, J. Jiang, et al. Chem. Soc. Rev., **42**, 2986 (2013).
[5] J. P Enriquez, Chalcogen. Lett., **10**, 45 (2013).
[6] Q. Li, B. Guo, J. Yu, et al. J Am. Chem. Soc., **133**, 10878 (2011).
[7] A. Hernández-Gordillo, F. Tzompantzi, R. Gómez, et al. Mater. Lett., **115**, 147 (2014).
[8] S. V. Kahane, R. Sasikala, B. Vishwanadh, et al. Int. J Hydrogen Energy, **38**, 15012 (2013).
[9] W. Zhu, X. Liu, H. Liu, et al. J Am. Chem. Soc., **132**, 12619 (2010).
[10] N. R. Mathews. Sol. Energy., **86**, 1010 (2012).
[11] K. Shin, S. I. Seok, S. H. Im, et al. Chem. Commun., **46**, 2385 (2010).
[12] S. U. Khan, M. Al-Shahry, W. B. Ingler, Jr. Science., **297**, 2243 (2002).
[13] G. K. Mor, O. K. Varghese, M. Paulose, et al. Sol. Energy Mater. Sol. C., **90**, 2011 (2006).
[14] I. Mora-Sero, S. Gimenez, F. Fabregat-Santiago, et al. Acc. Chem. Res., **42**, 1848 (2009).
[15] P. Sudhagar, J. H. Jung, S. Park, et al. Electrochim. Acta, **55**, 113 (2009).
[16] J. Bisquert . J Phys. Chem. B., **106**, 325 (2002).
[17] L. W. Chong, H. T. Chien, Y. L. Lee. J Power Sources, **195**, 5109 (2010).